Acoustic Emission Sensors Array for Concrete Structure Health Monitoring

Qiang WANG*, Qihua YANG*, Changmin YUAN*
* Dept. of Quality & Safety Engineering, China Jiliang University
Hangzhou 310018, China
qiangwang@cjlu.edu.cn

Abstract. Small size AE sensor array (circular and rectangle array) are developed to inspect internal defects. Beamforming offers a promising solution to AE array for large plate-like reinforced concrete structure structure health monitoring. Circular and rectangle array (8 elements) space directivity was compared. The conventional beamforming (CBF) and minimum variance distortionless response (MVDR) were separately used for AE signals direction-finding. The MVDR algorithm has higher angle resolution and lower sidelobe than CBF algorithm. The experiment was implemented on a concrete board. In limited area (radius is 3 meter), the results show that the CBF is unable to discriminate the direction of damaging AE signal, and MVDR based on UCA and URA clearly achieve the incidence angle of the broad band AE signal. The angular deflection was limited in 2-5° with actual AE direction.hese instructions are designed for the author and/or typist. They should be read carefully. If they are not adhered to, it may lead to a delay in publication and suboptimal reproduction quality. The document itself can be used as word template.

Introduction

Inspections on the current state of existing concrete structures have been increasingly carried out all over the world. Development and establishment of innovative and highly advanced non-destructive testing (NDT) are necessary [1-3]. The technique of infrared thermography has been successfully applied in a number of other areas applications—concrete structures and on highway bridges [4]. Elastic wave parameters such as velocity and attenuation are quite sensitive to the existence of damage, either in the form of distributed micro-cracks, which are considered suitable for characterizing damage in concrete [5]. Contactless recognition of concrete surface damage technique is developed based laser scanning [6]. Furthermoer, the radar and the Stack imaging of spectral amplitudes techniques are applied to on-site measurement in concrete structures [7].

Acoustic emission techniques has been used for years as a method for passive structural health monitoring, such as bridge concrete deck [8-9]. A conventional acoustic emission (AE) setup consists of many sensors distributed around potential source locations [8]. Traditional AE source localization method are relying on accurate arrival time detection algorithms requiring exact time synchronization of the data acquisition system and sensors [9-11]. Beamforming acoustic emission is a cost effective and elegant method of obtaining quantitative information from acoustic emission signals from one or more small arrays of 4-8 elements. The time delay beamforming had been applied to the method of acoustic emission by McLaskey in 2010 [12].

In this paper, the AE array (circular and rectangle) azimuth finding performance by performing beamforming for structure health monitoring was discussed. The 8-element

License: http://creativecommons.org/licenses/by/3.0/

planar array was designed to improve system azimuth finding performance. Combined with concrete AE source characteristics, conventional beamforming (CBF) and minimum variance distortionless response (MVDR) for AE arrays application are tested in simulation and experiment.

2. Circular and rectangle array Signal Model

1.1 Circular Array

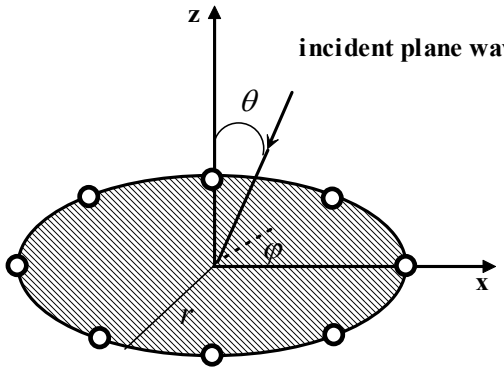

Fig. 1 Geometric configuration and coordinate system for circular array

For a uniform circular array (UCA) of radius r with N sensors, symmetrically placed on the circumference, see Fig.1. Let a plane wavefront be incident on the receiving array at azimuth angle θ_s and elevation angle ϕ_s . The beamforming of UCA is presented as [14]:

$$B_{cir}(\theta,\phi)=\sum_{n=0}^{N-1} w(\phi_n)s(t)\exp\left[j\frac{2\pi}{\lambda}\sin\theta_s\cos\left(\phi_s-\phi_n\right)\right] \qquad (1)$$

For CBF, the $w\left(\phi_n\right)$ is set as :

$$w\left(\phi_n\right)=\mathrm{e}^{-j\frac{2\pi}{\lambda}R\sin\theta_s\left[\cos\left(\phi_s-\phi_n\right)\right]} \qquad n=1,2,\cdots,N \qquad (2)$$

1.2 Rectangle Array

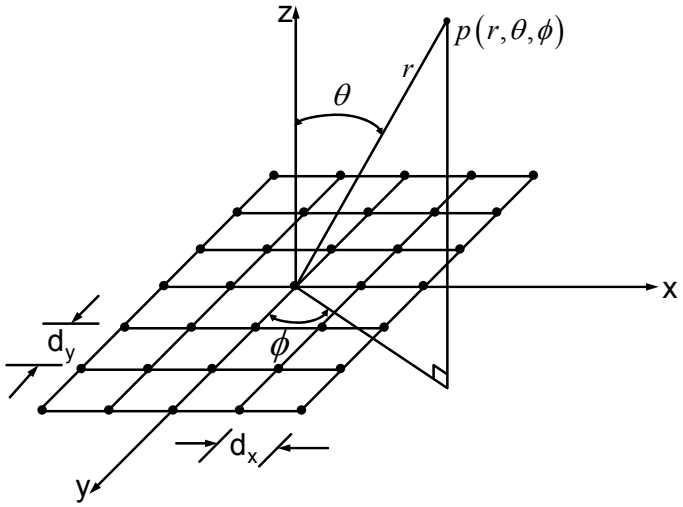

Fig. 2. Configuration and coordinate system for rectangle array

For $M\times N$ identical elements with uniform spacing placed on the x-y plane, as shown in Fig. 2, the beamforming of uniform rectangle array(URA) is presented as [13]:

$$B\left(\psi_x,\psi_y\right)=\sum_{n=1}^{N}\sum_{m=1}^{M}w_{mn}s\left(t\right)\mathrm{e}^{j\left((n-1)\psi_x+(m-1)\psi_y\right)} \qquad (3)$$

$\psi_x=\frac{2\pi}{\lambda}d_x\sin\theta\cos\phi$, $\psi_y=\frac{2\pi}{\lambda}d_y\sin\theta\sin\phi$, and w_{mn} represents the weight of the individual elements.

1.3 DOA Estimation of AE Array

The purpose of beamforming is to find a group of weighted vectors to combine sensors in the way where signals at particular angles experience constructive interference and while others experience destructive interference.

The output of an array can be expressed as:

$$y\left(t\right)=\sum_{i=1}^{M}w_i^{*}x_i\left(t\right)=\boldsymbol{w}^{\mathrm{H}}\left(\phi\right)\boldsymbol{x}\left(t\right) \qquad (4)$$

where

$$\boldsymbol{x}(t)=\left[x_1(t)\quad x_2(t)\quad\cdots\quad x_M(t)\right]^{\mathrm{T}},\ \boldsymbol{w}(\phi)=\left[w_1(\phi)\quad w_2(\phi)\quad\cdots\quad w_M(\phi)\right]^{\mathrm{T}}$$

M denotes the number of the array, $x_i(t)$ is the signals achieved by the sensor, $w_i(\phi)$ is the weight of each sensor.

The whole beamforming output power of the array (azimuth spectrum) is given by:

$$P_{CBF}\left(\phi\right)=\boldsymbol{w}^{\mathrm{H}}\left(\phi\right)\boldsymbol{R}\,\boldsymbol{w}\left(\phi\right) \qquad (5)$$

where $\boldsymbol{R}=E\left[\boldsymbol{x}\left(t\right)\boldsymbol{x}^{\mathrm{H}}\left(t\right)\right]$ is the covariance matrix of the $\boldsymbol{x}(t)$.

For MVDR beamformer, it minimizes the mean output power of the noise and interference while passing signals from the steered direction [13]. The azimuth spectrum of MVDR is given by

$$P_{MVDR}=\frac{1}{\boldsymbol{a}^{\mathrm{H}}\left(\phi\right)\boldsymbol{R}^{-1}\boldsymbol{a}\left(\phi\right)} \qquad (6)$$

3. Simulation Test

In simulation testing, a standard circle array (small size, diameter is 60 mm) and the rectangular AE array (d_x=d_y=15mm) with 8 elements are designed. Concrete AE signal center frequency is 75 kHz, wave velocity is about 2500 m/s.

Simulations were performed to verify whether the UCA and URA beampattern in the azimuth plane for different steering angles. In Fig. 3 (assuming angle ϕ is 100°), it is clear to know that UCA has higher angle resolution and lower side-lobe level than URA. Furthermoer, we compare the direction-finding performance of CBF algorithm and MVDR algorithm based on UCA and URA in Fig. 4 (assuming angle ϕ is 90°).

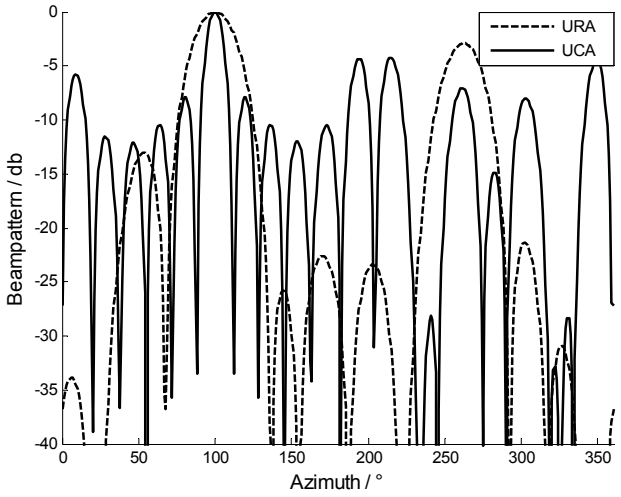

Fig. 3. Beampattern of 8 element circle array and rectangular array

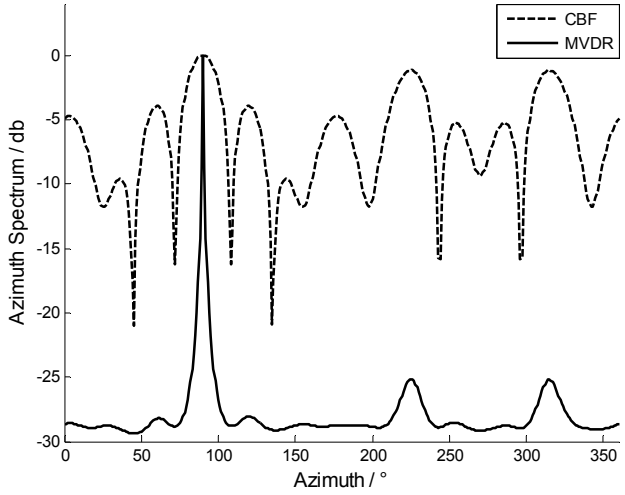

(a) The direction-finding result with CBF and MVDR based on UCA

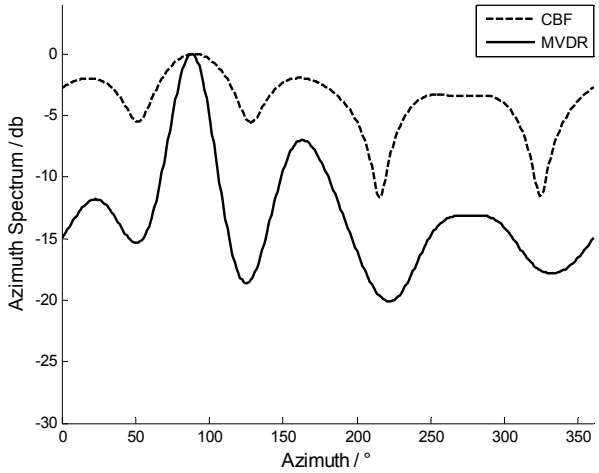

(b) The direction-finding result with CBF and MVDR based on URA

Fig. 4. Direction finding comparison of UCA and URA array

In the Fig. 4, it is shown the CBF is not able to accurately estimate the incident direction of the AE source owing to the influence of grating lobes. But for MVDR, there exists one main peak, it is easy to identify the incident AE source azimuth angle (90°) for UCA, URA. Compared MVDR results of two arrays, the UCA has narrower main beamwidth. Therefore it has the higher spatial resolution and lower the side-lobe level than

the URA. The UCA achieves deeper nulls toward other signals, that is to say the UCA has stronger interference rejection capability to noises and interference signals from other direction compared to the URA.

4. AE Direction Finding of Experimental Data

4.1 AE Signal Characteristics

A concrete structure pencil break test was conducted on a concrete deck (height is 0.2 m, testing area radius is 3 m). The acoustic emission SAMOS system (from Physical Acoustics Corporation) was used to gather AE signal for off-line beamforming analysis. Using the pencil lead fracture, the AE wave average velocity of 10 times was measured 2851.5 m/s, it belongs to Rayleigh wave field.

The typical concrete AE signal was presented in Fig. 5. The AE damaging source signal energy was focused on the range from 0 kHz to 100 kHz. The signal's main energy breaks time at 200~500 μs. With the anti-alias filtering, the band limited AE signals which have propagated through concrete facilitates the use of lower sampling rates (50kHz).

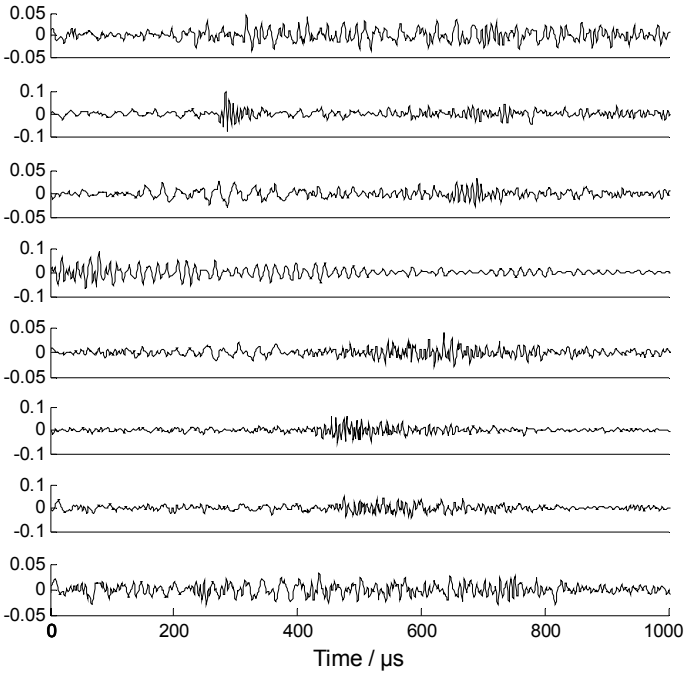

Fig. 5 The concrete acoustic emission signals of 8 channel

4.2 Direction finding results of test

In the experiment, the target AE source was generated at 90° to the array (distance is 3 meter). We compared the directivity patterns of two array architectures discussed above. The azimuthal direction of arrival the AE waves was estimated by finding the maximum of power-versus-azimuth curve in Fig. 6. The curve was calculated for steered azimuths equally spaced over the entire range from 0°~360°. Though AE array size is small, the direction of arrival also meet practical requirement.

The direction-finding results are presented in Figure 6 and Figure 7. It is clear that CBF is unable to discriminate the AE source azimuth angle based on UCA and URA. In Fig.

6(a) and Fig.7(a), the maximum sidelobe of two array is about -13 dB, -7 dB respectively. The target source is covered by environment noise.

In Fig. 6(b), though the DOA of incident wavefronts is unknown, the UCA also gain good wideband focusing effect. It is can be seen that the URA is unable to gain good angle directivity. The sidelobes in Fig 7(b) could not be suppressed to the desired value. Compared Fig.6(b) with Fig.7(b), the MVDR spectrum based on UCA gains better direction-finding results than URA. The actual peaks are discriminated at 88°, the error is about 2°. And there exists no grating lobe. Figure 7 shows that the direction-finding result with MVDR based on URA is 103°, the angle error is 13°, furthermore, there exists several grating lobes. Therefore, the MVDR based on UCA has higher accuracy and higher angle resolution than URA.

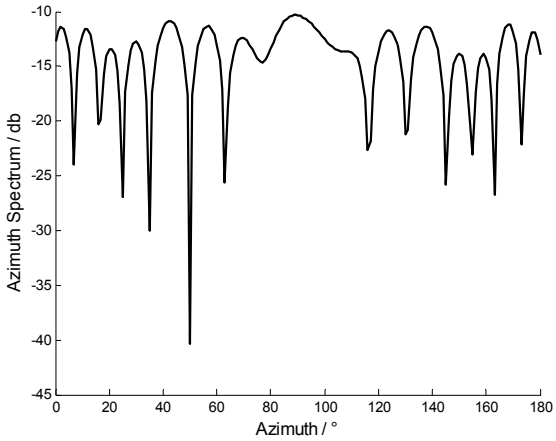

(a)CBF AE source direction finding results with UCA

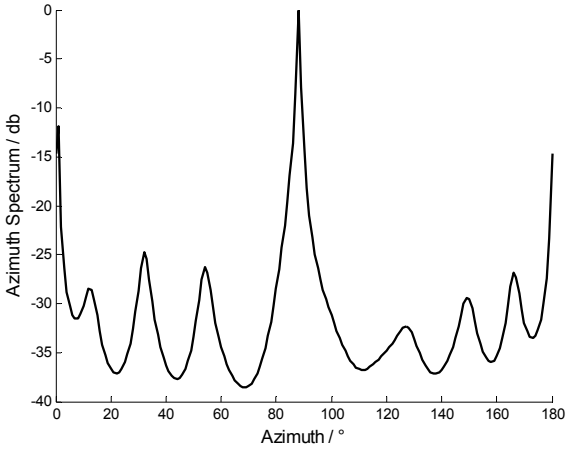

(b)MVDR AE source direction finding results with UCA

Fig. 6 The Direction finding results of CBF and MVDR spectrum with UCA

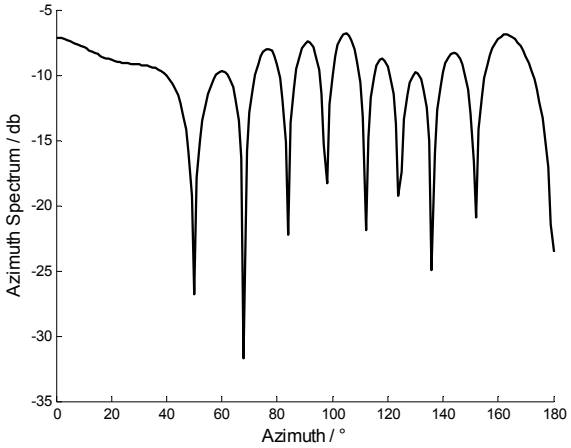

(a) CBF AE source direction finding results with URA

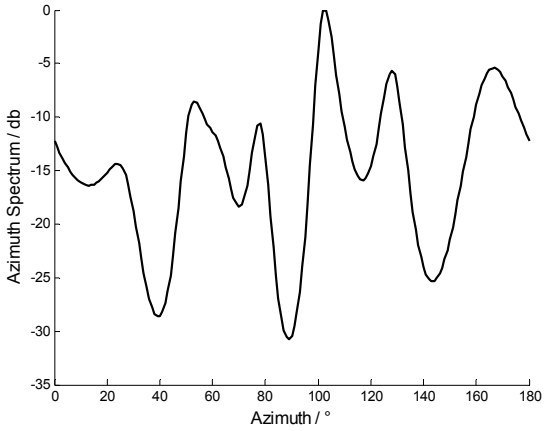

(b) MVDR AE source direction finding results with URA

Fig. 7 The Direction finding results of CBF and MVDR spectrum with URA

5. Conclusion

In this study, the small scale experiments show the ability of the small-size AE array combined MVDR to monitor concrete internal broad band AE source in reinforced concrete structure. For an eight element circular and rectangular AE array, the MVDR and CBF angle spectrum are compared with test data. The MVDR for UCA gain better DOA performance than CBF for concrete damaging broad band AE source (10kHz~100kHz). The techniques can be applied to small size wireless AE array for real time AE source localization. Experiment results future applicability may be performed in non destructive testing of large concrete structures in-situ and in modelling fractured media response to long time dynamic loading.

Acknowledgment

The work was supported by National Science Foundation of China under Grant 51275498, Zhejiang Provincal National Science Foundation of China under Grant Y1100096.

References

[1] D. A. Sack and L. D. Olson, “Advanced NDT methods for evaluating concrete bridges and other structures,” NDT & E International, vol. 28, no. 6, pp. 349-357, Dec. 1995.

[2] Kentaro Ohno, Masayasu Ohtsu, Crack classification in concrete based on acoustic emission," Construction and Building Materials, vol. 24, no. 12, Dec 2010, pp. 2339-2346.
[3] D. M McCann and M.C Forde, "Review of NDT methods in the assessment of concrete and masonry structures," NDT & E International, vol. 34, no. 2, pp. 71-84, Mar 2001.
[4] M. R. Clark, D. M McCann, and M. C. Forde, "Application of infrared thermography to the non-destructive testing of concrete and masonry bridges," NDT & E International, vol. 36, no. 4, pp. 265-275, Jun 2003.
[5] D. G. Aggelis, E. Z. Kordatos, M. Strantza, D. V. Soulioti, T.E. Matikas, "NDT approach for characterization of subsurface cracks in concrete," Construction and Building Materials, vol. 25, no. 7, pp. 3089-3097, Jul 2011.
[6] G. Teza, A. Galgaro, and F. Moro, "Contactless recognition of concrete surface damage from laser scanning and curvature computation," NDT & E International, vol. 42, no. 4, pp. 240-249, Jun 2009.
[7] K. Matsuyama, M. Yamada, and M. Ohtsu, "On-site measurement of delamination and surface crack in concrete structure by visualized NDT," Construction and Building Materials, vol. 24, no. 12, pp. 2381-2387, Dec 2010.
[8] C. U. Grosse, M. Ohtsu (Eds.). Acoustic Emission Testing in Engineering - Basics and Applications. Springer publ., Heidelberg , 2008.
[9] C. U. Grosse, "Acoustic emission localization methods for large structures based on beamforming and array techniques," NDTCE'09, Non-Destructive Testing in Civil Engineering, Nantes, France, June 30th – July 3rd, 2009.
[10] T. Lokajíček , K. Klíma, "A first arrival identification system of acoustic emission (AE) signals by meansof a high-order statistics approach," Measurement Science and Technology, vol. 17, pp. 2461–2466, 2006.
[11] S. J.Spencer, "The two-dimensional source location problem for time differences of arrival at minimal element monitoring arrays," The Journal of the Acoustical Society of America, vol. 121, pp. 3579-3594.
[12] G. C. McLaskey, S. D. Glaser and C. U. Grosse, "Beamforming array techniques for acoustic emission monitoring of large concrete structures," Journal of Sound and Vibration, vol. 329, pp. 2384 – 2394, 2010.
[13] D. H. Johnson, D. E. Dudgeon, Array Signal Processing: Concepts and Techniques, Prentice-Hall PTR: Englewood Cliffs, NJ, 1993.
[14] Q. Wang, X. Liu, "Acoustic Emission Sensors Circular Array for Concrete Structure Damaging Source DOA Estimation", Proceedings of the Eighth International Workshop on Structural Health Monitoring, Editor: Fu-Kuo Chang, pp 2189-2194, 2011.